Science of the Total Environment 747 (2020) 141272

Contents lists available at ScienceDirect

Science of the Total Environment

journal homepage: www.elsevier.com/locate/scitotenv

Compound flooding in Houston-Galveston Bay during Hurricane Harvey

Arnoldo Valle-Levinson [a,*], Maitane Olabarrieta [a], Lorraine Heilman [b]

[a] Civil and Coastal Engineering Department, University of Florida, Gainesville, FL 32611, United States of America
[b] Center for Operational Oceanographic Products and Services, National Ocean Service, NOAA, Silver Spring, MD 20910, United States of America

HIGHLIGHTS

- An early-August storm increased susceptibility of Houston to flooding from Harvey.
- Harvey flooded Houston via two sources of runoff: San Jacinto and Buffalo Bayou.
- Flooding was worsened by 3 factors a) phase lag between the two sources of runoff
- b) 2 coastline constrictions, and c) ocean-derived forcing: surge & mean sea level

GRAPHICAL ABSTRACT

The extreme flooding from Hurricane Harvey around Houston in late August 2017 was linked to compound flooding. Storm surge from the ocean provided the first punch, Buffalo Bayou discharge represented a second punch, and San Jacinto River discharge inflicted a 3rd punch.

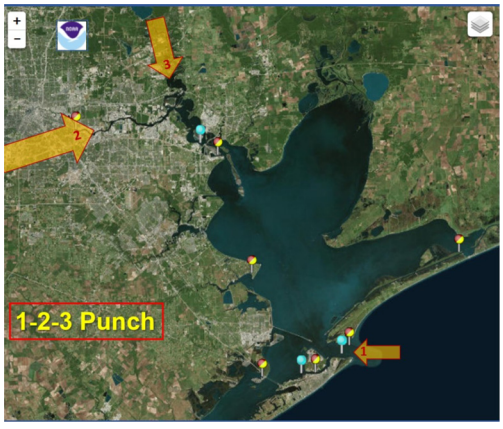

ARTICLE INFO

Article history:
Received 16 June 2020
Received in revised form 22 July 2020
Accepted 24 July 2020
Available online 25 July 2020

Editor: Fernando A.L. Pacheco

Keywords:
Compound flooding
River flooding
Storm surge
Hurricane Harvey

ABSTRACT

Hurricane Harvey reached Category 4 when it made landfall on the coast of Texas in late August 2017. Harvey not only affected the coastal region with wind speeds that peaked near 50 m/s, it also dumped ~7.6×10^{10} m^3 of rain over 3 days. This rainfall was equivalent to the discharge of the Amazon River over the same period and made Harvey the wettest tropical cyclone to affect the United States. Winds and rainfall interacted to produce atypical storm surges along the coast and estuaries of Texas and compound flooding in the Houston region. Data from the NOAA's Center for Operational Oceanographic Products and Services provided information on water levels in this region. The highest water levels, 3 m above predicted, occurred from August 27th to 29th at Buffalo Bayou in the uppermost reaches of the Galveston-Trinity-Tabbs-Burnet Bay system. The peak surge occurred on Aug 29th because of the triple punch of a) the ocean wind stress and corresponding surge, plus the rainfall-related land-derived discharge from b) Buffalo Bayou and then from c) the San Jacinto River. Winds from the ocean persisted during that 3-day period and drove onshore water transport. This transport, together with anomalously high mean sea levels and the coastline modifications in the upper bay system, delayed the seaward motion of the land-derived discharge. Numerical model simulations that turned forcings on and off, highlighted the importance of the two river pulses in causing the widespread flooding. Simulations also underscored the influence of the interaction between land-derived discharge and ocean-derived surge along different parts of the Houston-Galveston Bay system.

* Corresponding author.
E-mail address: arnoldo@ufl.edu (A. Valle-Levinson).

https://doi.org/10.1016/j.scitotenv.2020.141272

1. Introduction

When a cyclone affects coastal areas, it is likely to drive water levels up on the side of the storm where winds are predominantly onshore. This process, also referred to as a storm surge, happens in tropical and extratropical cyclones and has been documented extensively (e.g. Cho et al., 2012; Li et al., 2006; Park et al., 2007). Storm surges can impact coastal regions through flooding of ocean waters. However, coastal flooding can also occur from land-derived freshwater pulses when a storm unloads anomalously high amounts of rain. For instance, a northeast monsoon in India caused catastrophic flooding in the Coromandel coast of South India, in December 2015. The La Niña event of 2010–2011 brought analogous rain-related flooding in Brisbane, Australia. Similarly, widespread flooding in coastal cities throughout the United Kingdom occurred in June–July 2007.

There are instances when the storm surge from the ocean combines with heavy precipitation from the storm to compound the flood (Leonard et al., 2014). In compound flooding, the combination of hazards causes more severe damage than that resulting separately from either source (Wahl et al., 2015; Zscheischler et al., 2018; Bevacqua et al., 2019). In fact, there seems to be an increase in compound flooding over the last five years, following the 20th century trend for an increase in 'great floods' (Milly et al., 2002) because of global warming (Bevacqua et al., 2019). The above authors have projected a continuation of the increasing trend for catastrophic floods, which seems to be holding. The highest probability of compound flooding is occurring presently in Mediterranean coastal regions and is expected to develop in the near future in northern Europe (Bevacqua et al., 2019). Further assessments have also explored compound flooding potential at global scales (Cousanon et al., 2020) and at scales of specific sites (e.g., Zhang et al., 2020; Ye et al., 2020). Different approaches to the compound flooding problem have included three-dimensional numerical models from creeks to ocean (Zhang et al., 2020; Ye et al., 2020), probabilistic simulations combined with one-dimensional models (Serafin et al., 2019) and Bayesian networks (Cousanon et al., 2018).

In the eastern United States coastal region, the trend for increased compound flooding has also been evident. In only three years, between 2016 and 2018, there were at least four dramatic events of compound flooding. In 2016, Hurricane *Matthew*'s rains and storm surge flooded the historic city of Saint Augustine in Northeast Florida. The following year, Hurricane *Harvey* caused widespread compound flooding in the Houston area in late August 2017. In the same year, a mere two weeks later, Hurricane *Irma* drove compound flooding in Jacksonville, Florida, in mid-September. Hurricane *Florence* slammed the coasts of North Carolina and South Carolina in September 2018, causing extensive flooding along coastal regions and at inland locations (Gori et al., 2020). Recent studies have described the effects of *Harvey* on the flushing and recovery of hydrographic properties in Galveston Bay (Du and Park, 2019), as well as its effects on sedimentation processes (Du et al., 2019). The purpose of this study is to understand the details that caused widespread compound flooding by *Harvey* in the Houston area. This hurricane is the wettest storm in the history of the United States, causing persistent flooding in the region for 3–8 days. The objective of studying compound flooding is pursued with data available from the National Oceanic and Atmospheric Administration (NOAA) and the United States Geological Survey (USGS) stations, combined with numerical simulation results.

2. Hurricane *Harvey*

Hurricane *Harvey* started as an atmospheric tropical wave that was conspicuous between western Africa and the Caribbean on August 16–17, 2017. In its westward translation, the tropical wave evolved to depression and tropical storm *Harvey* on August 17th. By August 19th it degenerated back to a tropical wave north of the Guianas. On August 19th and 20th, the tropical wave moved across the Caribbean, and on August 21–22 crossed over the Yucatan Peninsula (Fig. 1a). The wave reformed into a tropical depression as it entered the Gulf of Mexico on August 23rd. On its northward translation in the Gulf of Mexico, the depression became a Category 4 hurricane by August 24th. The hurricane then veered northwestward to make landfall on Aug 26th, stalling and weakening to a tropical storm near Port Aransas and the Aransas Wildlife Refuge in Texas (Fig. 1b). Instead of continuing a landward trajectory on August 26th, the hurricane eye slowly looped cyclonically late on August 26th and on the 27th, dropping heavy rains for two days. On August 28th, the storm moved seaward from land and re-entered the Gulf of Mexico, near Matagorda City, Texas. The hurricane crawled nearly parallel to the coast until another landfall on Aug 30th on western Louisiana. During the slow-moving period, between Aug 26th and 30th, the hurricane dumped more than 1.5 m of rain in some areas around Houston. The hurricane caused the largest tropical rainfall in the history of the US. The slow motion of the storm unloaded ~9.3×10^{10} m^3 of water over 5 days in Texas and Louisiana (Fritz and Samenow, 2017) and built a storm surge on the coastal ocean. Seaward moving pulses from land drainage and the landward pulse from the ocean combined to promote widespread flooding in the region (Emanuel, 2017), particularly in the city of Houston.

3. Physical setting: Houston- Galveston Bay

The morphology of the Houston-Galveston Bay region (Fig. 2) exacerbated the flooding caused by the storm surge from the ocean and by the storm-related pluvial precipitation on land. The city of Houston is connected to the Gulf of Mexico through an intricate system of bayous, rivers and bays that open up to Galveston Bay (Fig. 2a). Rain-related flooding in Houston may occur from two main rivers, among other bayous, marshes and creeks: San Jacinto River and Buffalo Bayou. The San Jacinto is formed by outflows from Lake Houston, which is ~30 km to the NE of downtown Houston. Buffalo Bayou, also known as Houston Ship Channel, is a stream that flows east-southeastward through downtown Houston. Buffalo Bayou meets the San Jacinto River (Fig. 2) at a 300 m constriction, just north of Burnet Bay. Going seaward, Burnet Bay and a complex system of sub-bays that are interrupted by islands is separated from Tabbs Bay by a 400 m constriction, at the Fred Hartman bridge crossing of State Highway 146 S (Fig. 2). Moving further seaward, Tabbs Bay widens out through two openings to Galveston and Trinity bays, which expand to ~37.5 km across and represents the upper part of Galveston Bay. A constriction of ~13 km separates Galveston Bay from north to south. In turn, Galveston Bay expands parallel to the coast for ~80 km and connects to the ocean mainly through two inlets. The direct connection to Galveston Bay is a 2.5 km inlet to the north of the city of Galveston (Fig. 2). The second inlet is San Luis Pass, off the southwestern extension of Galveston Bay, also known as West Bay.

The two largest constrictions from Houston to Galveston Bay: a) between the San Jacinto-Buffalo Bayou confluence and Burnet Bay; and b) between Burnet Bay and Tabbs Bay (Fig. 2) are crucial for the seaward drainage of land-derived discharges from the San Jacinto River and Buffalo Bayou. The two constrictions represent bottlenecks for the seaward flushing of floodwaters around Houston. As described in this study, these were choke points during Hurricane Harvey that exacerbated the flooding by providing a 1–2 punch (Buffalo Bayou-San Jacinto) to flooding the city of Houston. The relatively narrow connection to the ocean at the city of Galveston provided a third choke point in the nexus streams – ocean, as detailed next.

4. Water level surges throughout the system

4.1. South of Houston-Galveston Bay

Before affecting the area of Houston, Hurricane *Harvey* propelled storm surges throughout southern coastal Texas as recorded by NOAA tide gauge stations. The lower Corpus Christi Bay was affected early on

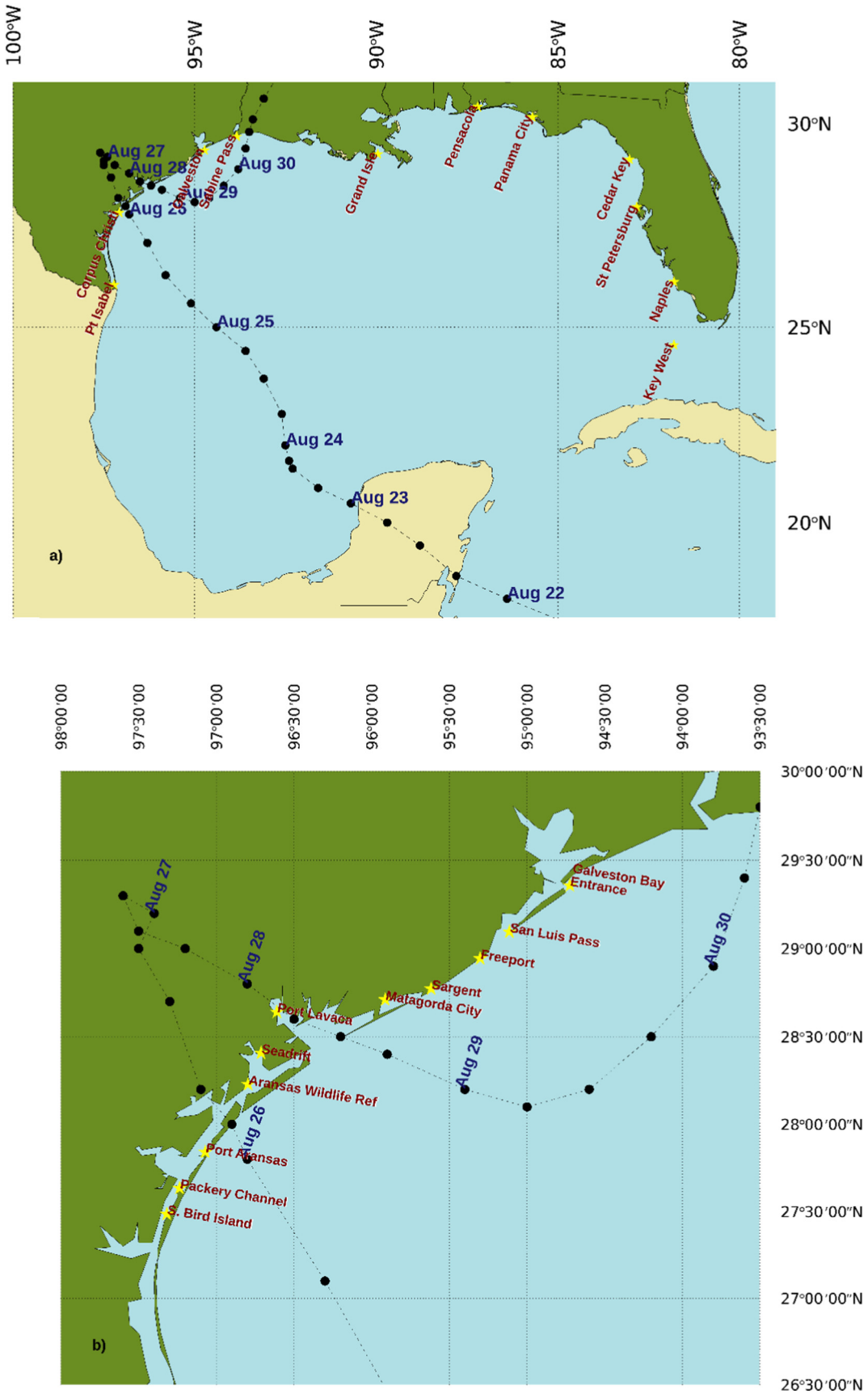

Fig. 1. Hurricane Harvey trajectory in the Gulf of Mexico (a), and zooming into the area south of Galveston Bay, where it made landfall.

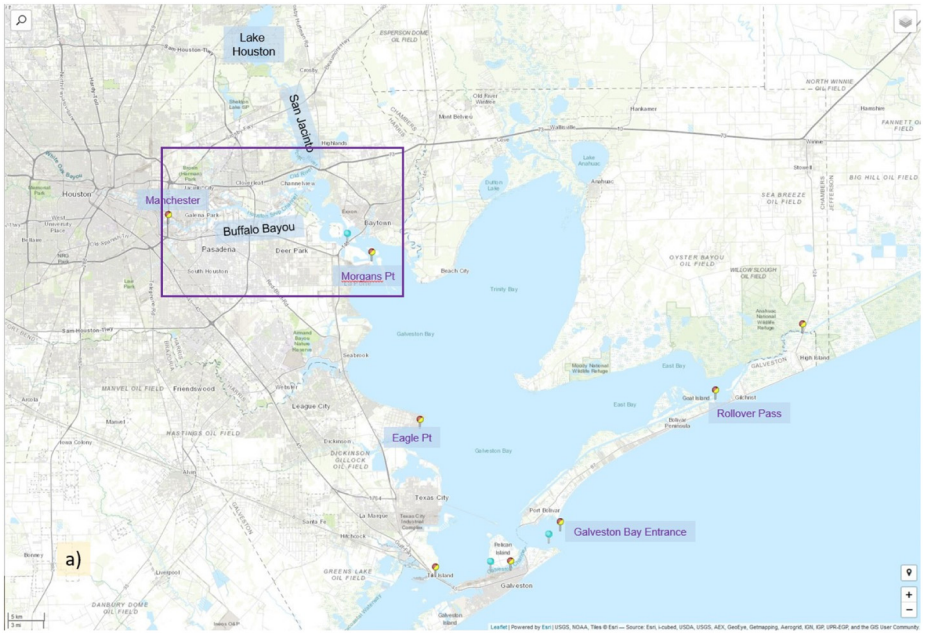
Lake Houston
San Jacinto
Manchester
Buffalo Bayou
Pasadena
Morgans Pt
Eagle Pt
Rollover Pass
Galveston Bay Entrance
a)

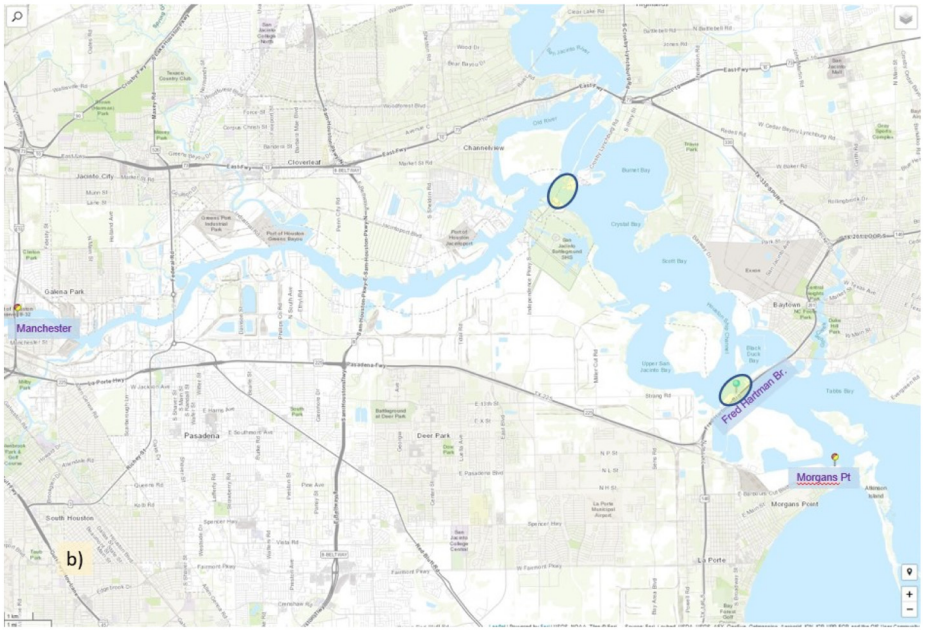
Manchester
Pasadena
Morgans Pt
Fred Hartman Br.
b)

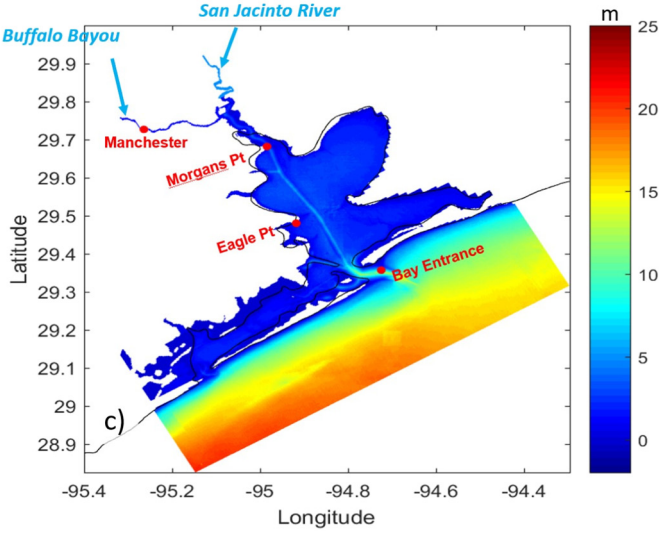
San Jacinto River
Buffalo Bayou
Manchester
Morgans Pt
Eagle Pt
Bay Entrance
c)
Latitude
Longitude
m
29.9
29.8
29.7
29.6
29.5
29.4
29.3
29.2
29.1
29
28.9
-95.4
-95.2
-95
-94.8
-94.6
-94.4
25
20
15
10
5
0

Aug 26 GMT with surges up to 1.7 m, as seen in Packery Channel and Port Aransas (Figs. 1b and 3). The surge affected South Bird Island, ~10 km south of the bay entrance, approximately one hour later. At the same time when the surge reached lower Corpus Christi Bay, it also impacted the adjacent lower San Antonio Bay, to the north, at Aransas Wildlife Refuge station. The surge then affected upper San Antonio Bay at Seadrift and upper Lavaca Bay at Port Lavaca, to the north, as the hurricane made landfall. Before reaching Houston, Hurricane *Harvey* caused the largest ocean surge (2 m) at Port Lavaca, likely a consequence of landfall and funneling effects in Lavaca Bay.

As the hurricane looped around inland, the storm surge also appeared on August 26th in Matagorda Bay, at Matagorda City and Sargent (Figs. 1b and 3). However, in contrast to the sites to the south and west, the surge here lasted for almost one week with values close to 1 m. On September 1st, the surge started decreasing monotonically until September 7th (not shown). Further north and east, the surge at the Freeport coastal station and in West Bay at San Luis Pass was similar in height to Matagorda Bay (Fig. 3). However, it lasted for 4 days with a steady decrease at Freeport, but a 2-day decrease and then another 1-day peak at San Luis Pass. The surge variations responded to the path of the hurricane as it moved onshore and then along the coast. The persistence of the surge in Matagorda Bay must have been caused by the ocean-driven surge, first, and then by runoff from the >1 m rains over 4 days (Aug 26th–29th) that affected these bays, thus compounding the flooding through a 1–2 punch, 1 from the ocean and 2 from the rivers and creeks. An analogous but much more dramatic response of compound flooding developed in the Galveston-Trinity-Tabbs-Burnet Bay system, extending to the city of Houston.

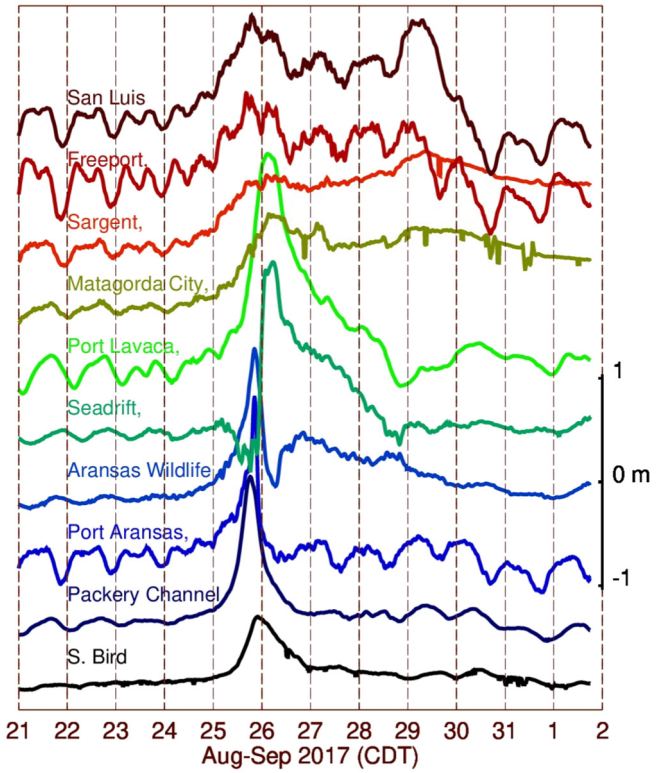

Fig. 3. Water levels over south Texas to the south of the Houston-Galveston Bay system during Hurricane *Harvey*. Records progress approximately northward from the bottom to the top in the figure (See Fig. 1b for station location) and are displaced vertically to distinguish each record. A common scale (in meters) for each record appears on the right vertical axis.

4.2. Around Houston

In early August, the western Houston area was affected by >0.15 m of rain that fell overnight on August 8th, causing widespread flooding as recorded by USGS gauges (Fig. 4a). To the east and north of the city (see records for Sims, Vince, Berry and Hunting Bayous in Fig. 4a), water levels rose suddenly and returned to pre-storm conditions by August 10th. However, the water level along Buffalo Bayou, the stream crossing Houston from west to east, remained above pre-storm values for nearly 2 weeks. These pre-*Harvey* conditions preconditioned the city of Houston for disastrous flooding during *Harvey*. When the hurricane affected the area, rapid surges in water elevation occurred in the bayous and creeks twice on August 26th (Fig. 4a, b). The second *Harvey*-related surge, late on August 26th to early August 27th, was more than twice larger than the earlier increase at Greens, Brays, Whiteoak, Sims, Hunting, Berry and Vince Bayous, as well as at Goose Creek (Fig. 4b). The expansive extent of the second surge on August 26th–27th, indicated flood outbreaks to Houston from the west, north and south, converging to Buffalo Bayou. These outbreaks receded differently in the southern bayous, Vince and Berry, compared to the floods to the north (Hunting) and west (Whiteoak, Brays and Sims, Fig. 4b). To the north, floods persisted for at least 4 days with a slow and monotonic withdrawal. In contrast, water levels to the south (Vince and Berry) retreated with oscillations and returned to near pre-storm values by the fourth day, on August 30th. The surge of water level late on August 26th was the first punch of flooding to the Houston area, after the preconditioning event on August 8th.

In contrast to the flooding along Buffalo Bayou, which occurred over ~3 h on August 26th–27th, the flooding further to the east in San Jacinto River developed over 3 days (Fig. 4b), from overflows at Lake Houston dam. At San Jacinto River, the water level increased almost steadily from August 27th to late August 29th, when it reached its peak. As the water level peaked in the San Jacinto River almost 3 days later than the peak in the city of Houston, waters from both flooding pulses converged at their confluence with Burnet Bay. Such convergence could have caused backflow toward the west, as San Jacinto's peak occurred later. At least, the pulse from San Jacinto River must have plugged or delayed Buffalo Bayou's flushing. It is evident that the broad pulse from San Jacinto River represented the second punch to Houston. Moreover, the constriction between Burnet Bay and Tabbs Bay, at the Fred Hartman bridge, must have delayed the flushing of both pulses from San Jacinto River and Buffalo Bayou. The third punch to the city of Houston came from the ocean-related storm surge in Galveston Bay.

4.3. Galveston Bay

Water levels at four NOAA stations in lower Galveston Bay remained anomalously high, ~0.8 m above expected tides, for nearly 5 days from August 25th to August 29th, 2017 (Fig. 5). The three stations closest to the inlet that communicates the bay with the ocean (Galveston Bay, Pier and Railroad) showed the same behavior without phase lags. The station in the lower bay, but on its eastern extreme, Rollover Pass, displayed similar behavior as near the inlet, but with a phase lag of nearly 4–5 h (Fig. 5). This phase lag, however, was consistent with the tidal phase lag between these two sites in the lower bay. Further into Galveston Bay, at Eagle Point, the surge increased to ~1 m and the tidal variations attenuated during the period of the surge. In the upper bay, Tabbs Bay at Morgans Point, the surge was similar to that in the middle bay at Eagle Point (Fig. 5). Tidal variations became even less apparent from August 28th to September 1st than in the mid-bay reaches. At the confluence of Buffalo Bayou and San Jacinto Rivers, at Lynchburg

Fig. 2. Houston-Galveston Bay system. a) Estuarine region showing the two main rivers that influence the city of Houston: Buffalo Bayou and San Jacinto. Also labeled are the NOAA tide stations. The rectangle indicates the region enlarged in b). b) Shows the confluence of the two rivers and the 2 constrictions (shaded ellipses) in the communication with Galveston Bay. In panels a) and b) northward is up. c) Numerical model domain.

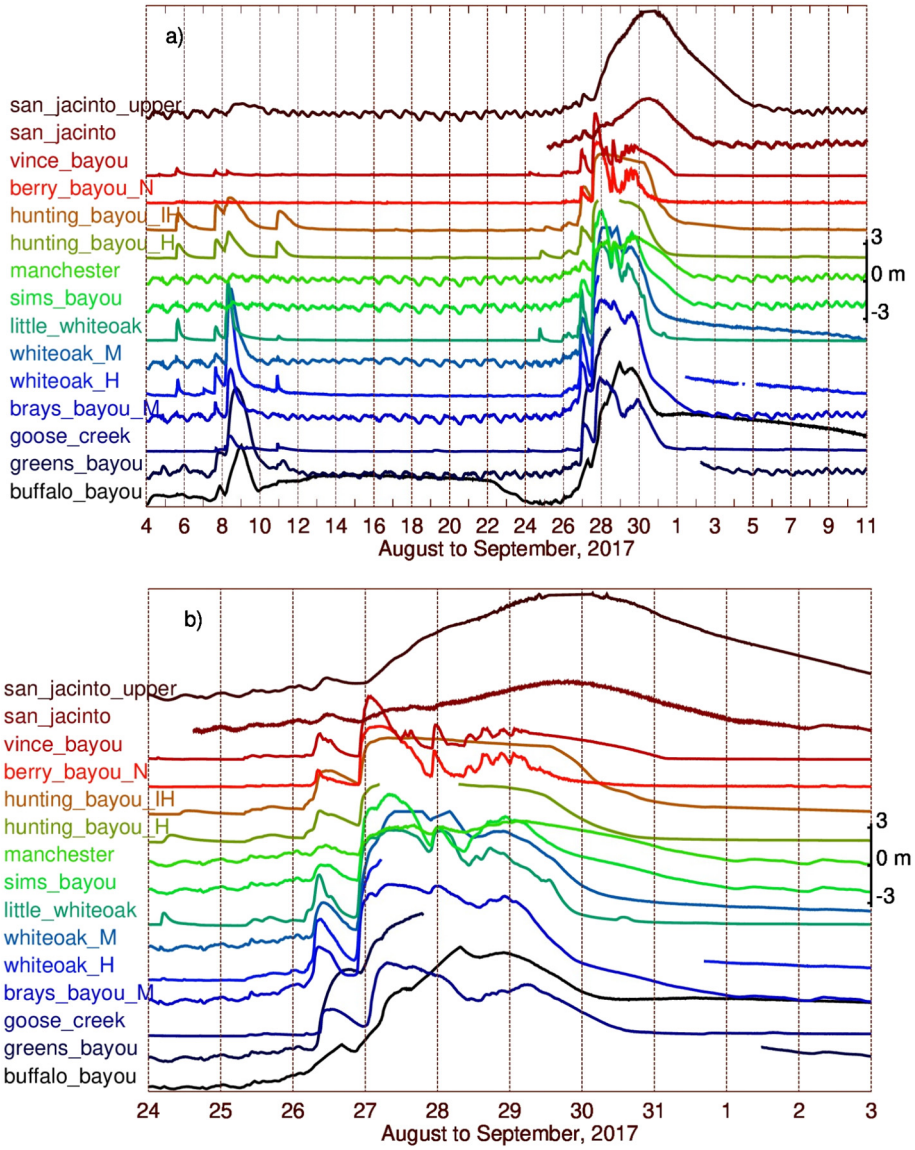

Fig. 4. Surge from river flooding in the Houston area (USGS stations). a) Forty days of water levels in the Houston area showing preconditioning for flooding from an early August's storm. b) Zoom in to the flooding from *Harvey*'s rains. Stations 'buffalo-bayou' and 'whiteoak_H' are to the west, while 'whiteoak_M' is in downtown; 'manchester' is to the east; 'brays_bayou_M' is to the south'; 'little_whiteoak' and 'hunting' are to the north; 'greens_bayou' is to the northeast; 'sims', 'berry' and 'vince' are to the southeast, beyond Rt. 610; 'goose_creek is to the east of San Jacinto and drains to Burnet Bay. All records are displaced vertically to distinguish each other. A common scale (in meters) for each record appears on the right vertical axis.

Landing, the surge increased dramatically to ~3 m early on August 29th. At the time of maximum surge, Lynchburg Landing station stopped recording and has been inactive since. It is likely that the San Jacinto River flooding caused the damage, as it occurred 2 days after a pulse further upstream in Buffalo Bayou at Manchester, which occurred late on Aug 26th to early on Aug 27th. Manchester station, inside the city of Houston, was NOAA's station in the Houston-Galveston Bay area that recorded the maximum surge, close to 3.5 m, on Aug 28th–29th, after the initial pulse on Aug 26th–27th. This second pulse at Manchester could have been related to i) backflow from the San Jacinto River that leaked past the constriction to Burnet Bay, or ii) blockage by San Jacinto River waters at the constriction. The direction of the flow at the lower and upper Galveston Bay provided further information on the processes that affected these water levels.

5. Flows at the river-estuarine-ocean transition

The flow at the entrance to Galveston Bay began showing the effects of the storm on August 25th, as inflows reached values close to 1 m/s (negative values, blue line on Fig. 6a). These relatively strong inflows developed despite being during equatorial tides, the weakest tides in a diurnally dominated fortnight. Ebb flows, or outflows, on this day reached values <0.3 m/s. This was the day when the water level began to increase in the lower bay. During the following day, August 26th, maximum ebb flows attained values of 1.6 m/s after the 0.8 m/s inflows early. Ebb flows persisted for the rest of the 26th in response now to the land-derived pulse associated with the storm rain. After a relatively weak inflow (<0.4 m/s) on August 27th, there was only outflow in the lower bay until September 1st (blue line, Fig. 6a). The outflow, however, still displayed tidal variations without reversing to inflow. This meant that there was so much land-derived water draining in the Houston-Galveston Bay nexus that there were 5 days without tidal inflow into Galveston Bay.

At the head of Galveston Bay, measurements from the Fred Hartman bridge showed attenuation, relative to the lower bay, of both tidal inflows and outflows before August 26th (amplitude of oscillations of red line < blue line, Fig. 6a). Beginning on August 26th, tidal inflows ceased because of drainage from the rivers, bayous and creeks from

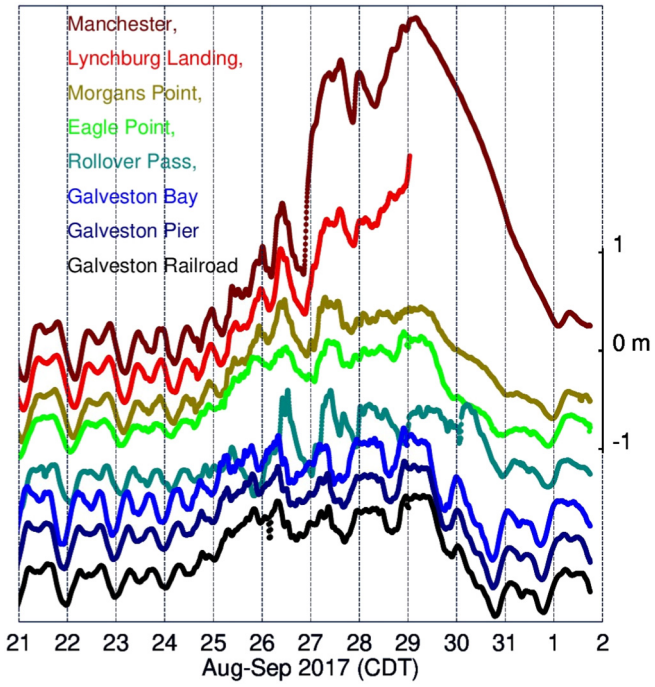

Fig. 5. Surge from ocean and flooding up estuary in Galveston Bay to Buffalo Bayou (NOAA stations). Manchester station is the same as in Fig. 4. See Fig. 2 for station positions. All records are displaced vertically to distinguish each other. A common scale (in meters) for each record appears on the right vertical axis.

the Houston area. In contrast to the lower bay, there were no tidal fluctuations appreciable in the outflow from August 27th to September 2nd. Tidal inflows in this part of the bay reappeared on September 4th, after nearly 8 days of only outflow. Tidal inflow cessation occurred for three more days than in the lower bay, indicating the land origin of the outward pulse. A daily index of landward amplification, same as seaward attenuation μ, was proposed to quantify these flow interactions, as follows:

$$\mu = sign[min(u_{mouth})]\left|\frac{min(u_{head})}{min(u_{mouth})}\right|, \quad (1)$$

which compared the daily minimum velocity at the head of the bay (u_{head}) to the daily minimum velocity at the lower bay (u_{mouth}). The μ coefficient shall conserve the sign of the minimum velocity at the lower bay. When the minimum velocity at the mouth was from tidal inflow, the μ value was negative. Seaward amplification or landward attenuation of tidal inflows occurs when $\mu < 1$. In periods with suppressed tidal inflow, the minimum velocity at the lower bay was positive (outflow) and μ values were positive, i.e., seaward attenuation or landward amplification of seaward currents developed when $\mu > 1$.

Before August 27th, the minimum velocities at the head and mouth of the bay were negative (tidal inflow, Fig. 6a) and μ was between −1 and 0 (Fig. 6b). This indicated that the tidal inflows were greater at the lower than at the upper bay, i.e., a landward attenuation of tidal inflows. Between August 27th and September 1st, when there was no tidal inflow in the lower bay, values of μ were >1, between 3 and 8. This indicated that ebb flows were 3 to 8 times greater in the upper than in the lower bay, i.e., seaward attenuation. By September 3rd, the behavior returned to landward attenuation of tidal inflows. The sign changes of μ values thus indicate the direction reversals of the predominant forcing, being landward on August 26th and becoming seaward from August 27th to September 1st.

The flushing efficiency of land-derived freshwater pulses toward the ocean was not only hindered by coastline constrictions in the upper Galveston Bay and by the ocean-related storm surge, it was also delayed by an increased baseline in sea level in the Gulf of Mexico. The year when Hurricane *Harvey* affected the northwestern Gulf of Mexico (2017), there was a peak in interannual variability of sea level in that part of the gulf (Fig. 7). This sea-level variability was consistent with that

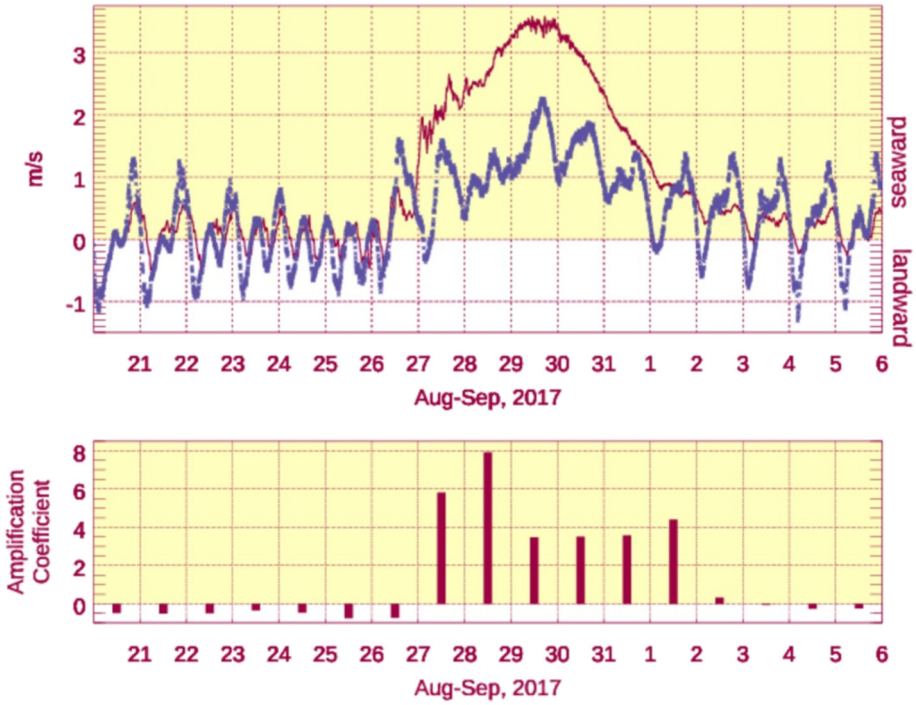

Fig. 6. Along-channel velocities at the upper and lower bay (NOAA stations), and corresponding amplification coefficient μ (see text for explanation of coefficient). a) Lower bay currents in blue and upper bay currents in red. Seaward flows are positive. b) Daily amplification coefficient calculated as in the text. Values <1 indicate landward attenuation of tidal currents. The sign of μ indicates the direction of flow in the lower bay at expected high tide, with positive values denoting no tidal inflow on that day.

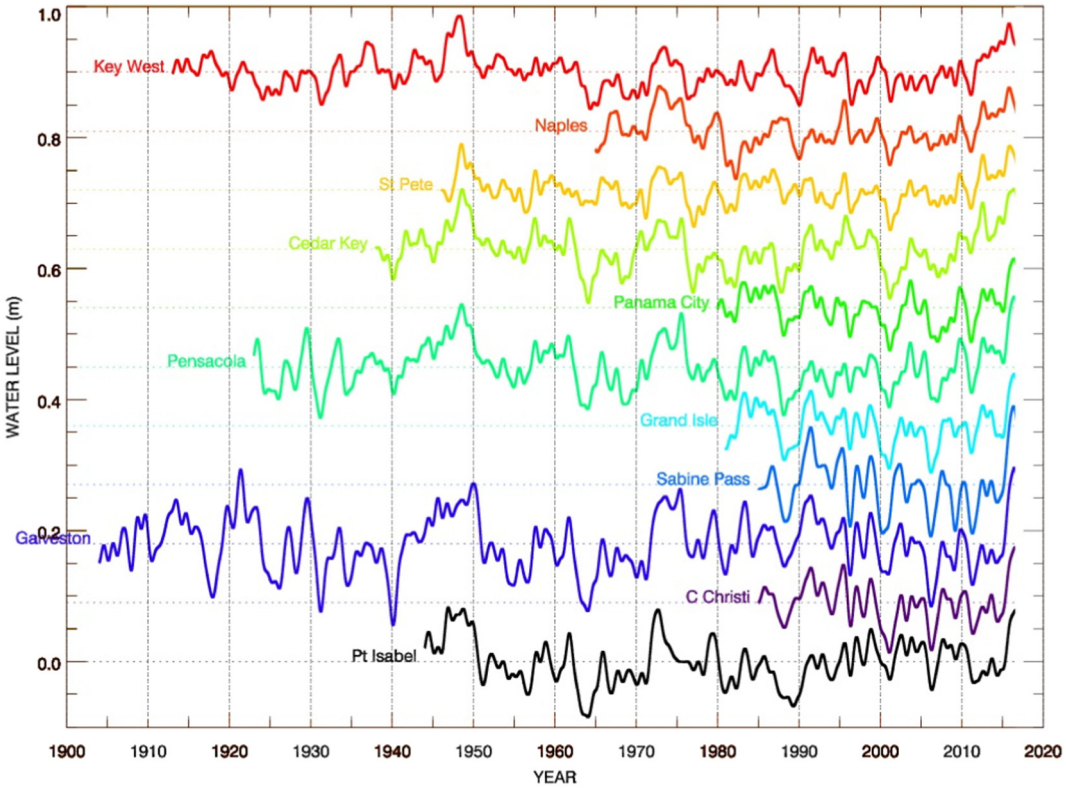

Fig. 7. One-year low-pass filtered and detrended sea levels around different NOAA sites in the Gulf of Mexico. The sites are shown in Fig. 1a. The figure illustrates a rapid increase of sea level in the Gulf of Mexico after 2015. Each record has been displaced vertically by 0.1 m to distinguish them from each other.

observed in the southeastern coast of the United States, from Cape Hatteras to the Florida Keys (Valle-Levinson et al., 2017). In the area of Galveston Bay, the mean sea level was 0.1 m higher than it was in 2011 (Fig. 7). Such sea-level increase of a few centimeters translated into a higher baseline upon which the storm surge and the land-derived pulses caused widespread flooding. It is likely that the ocean-derived and land-derived pulses were higher than the mere 0.1 m increase of baseline. This is because of the complex interactions between subinertial waves (e.g. Proudman, 1957; Horsburgh and Wilson, 2007; Valle-Levinson et al., 2013). Hence, the baseline increase during the year of *Harvey* was part of the third punch to affect the Houston area.

The baseline high stand reinforced the ocean-related surge to plug the land-derived volume excess, thus exacerbating the flooding throughout the northwestern Gulf of Mexico. The water level and current velocity data described above suggested the hypothesis of a 1-2-3 punch that compounded the flooding in the Houston-Galveston Bay area. A 1-2 punch appeared in the Buffalo Bayou and San Jacinto River discharge, while the third punch was in the form of an ocean plug caused by storm surge and mean sea-level increase. In other words, two punches from land plus one from the ocean compounded flooding. The hypothesis is discussed next with process-oriented numerical simulations in a geometry similar to that of the Houston-Galveston Bay area.

6. Discussion

This section presents numerical simulations geared toward testing the hypothesis that the anomalous flooding in the upper Galveston Bay and Houston area, related to *Harvey*, was compounded by a 1-2-3 punch: 1-2 from rivers and 3 from ocean. Numerical experiments were executed with the Regional Ocean Modeling System (ROMS) over a morphology that emulated Galveston Bay with the influence of two freshwater inputs (Fig. 2c). The ROMS is three-dimensional, terrain-following and solves finite-difference approximations of the Reynolds-Averaged Navier-Stokes equations with free surface. It uses the hydrostatic and Boussinesq approximations (Chassignet et al., 2000; Haidvogel et al., 2000) with a split-explicit time stepping algorithm (Shchepetkin and McWilliams, 2005; Haidvogel et al., 2008). The modeling grid had a horizontal resolution of 100 m in the meridional and zonal directions, plus three equally spaced vertical sigma layers. The bathymetry of the domain was derived from a NOAA inundation digital elevation map. Local wind and atmospheric pressure were provided to the model from the North Atlantic Mesoscale (NAM) reanalysis. Initial salinity and ocean temperature were provided by the COAWST (Warner et al., 2010) forecast run by USGS (https://reduceflooding.com/2019/11/13/aerial-photos-of-lake-houston-dam-dramatize-need-for-more-gates/). The ocean-related surge and astronomic tides were prescribed at open boundaries also from COAWST. River inputs were estimated for Buffalo Bayou and San Jacinto River on USGS water discharge observations. At Buffalo Bayou, discharge measurements were unavailable during the peak of the flood; these were estimated from the correlation between detided water levels and discharge, and then adjusted to match modeled water levels to observations.

Model results for water elevation were compared to data from four NOAA tide gauges in Galveston Bay: the lower bay, the mid-bay, the upper bay, and the stream that runs through Houston. Sequentially from the bay entrance, NOAA stations were Galveston Bay Entrance, Eagle Point, Morgans Point, and Manchester. In order to explore the importance of each forcing in the water elevation throughout the system, the reference simulation had every forcing prescribed: the two rivers, atmospheric forcing, and ocean forcing. Simulated water levels with every forcing had similar variability to observed water levels (Fig. 8). Reference values of RMSE helped determine the relevance of each forcing during the period August 24th to 31st. The temporal variability of water levels seems to have been best represented in the lower bay despite not showing the lowest RMSE values.

Eliminating the influence of one river (the San Jacinto River) from all forcings increased errors inside the bay and in the upper bay, but not at

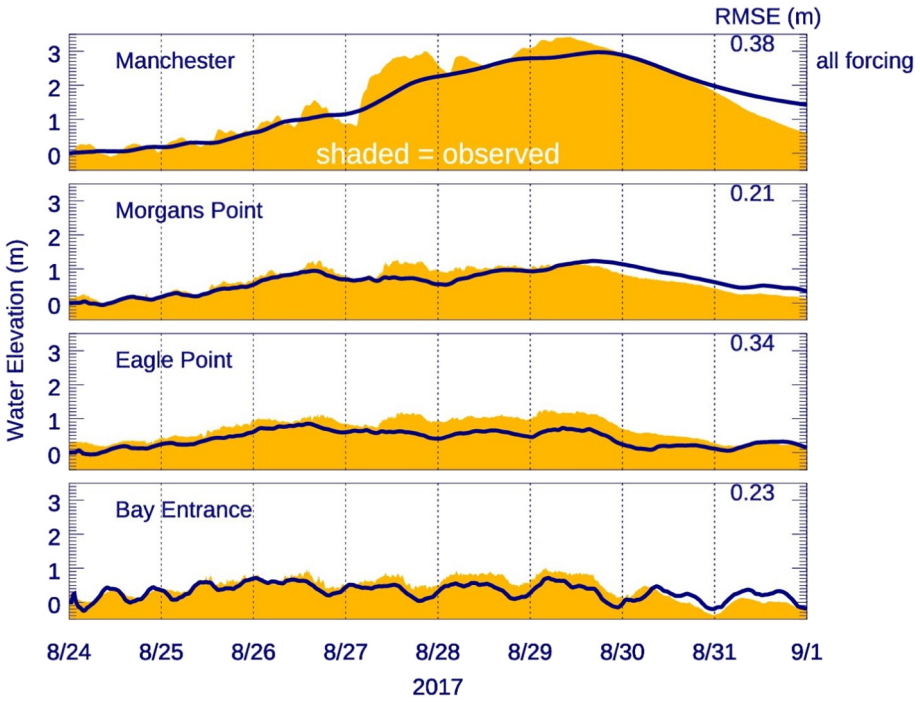

Fig. 8. Numerical results with every forcing active (lines) compared to observations at 4 NOAA sites (shaded). Values on the upper right of each frame indicate the root mean squared error between simulated and observed water levels.

the entrance (Fig. 9). In the area of Houston (Manchester station), inclusion of the San Jacinto was irrelevant until late August 28th. After that date, the San Jacinto maintained elevated water levels around Houston and in the upper bay (Morgans Point). Such effect was less effective, but still evident, in the middle bay (Eagle Point). Inclusion of one or two rivers was indistinct to the response at the lower bay (Bay Entrance). These results support the idea that flooding in Houston occurred first from the discharge at Buffalo Bayou and was compounded by the flooding from the San Jacinto River. Results underscore the importance of the two rivers in the flooding of the upper bay.

Elimination of river forcing altogether caused distinct water levels from those observed at the upper bay stations (Fig. 10). Until August 27th, water levels at all stations had negligible influence from river discharge. Up to that date, the storm surge from the lower bay must have increased water levels throughout. However, after August 26th the impact of rivers became evident at Manchester and Morgans Point

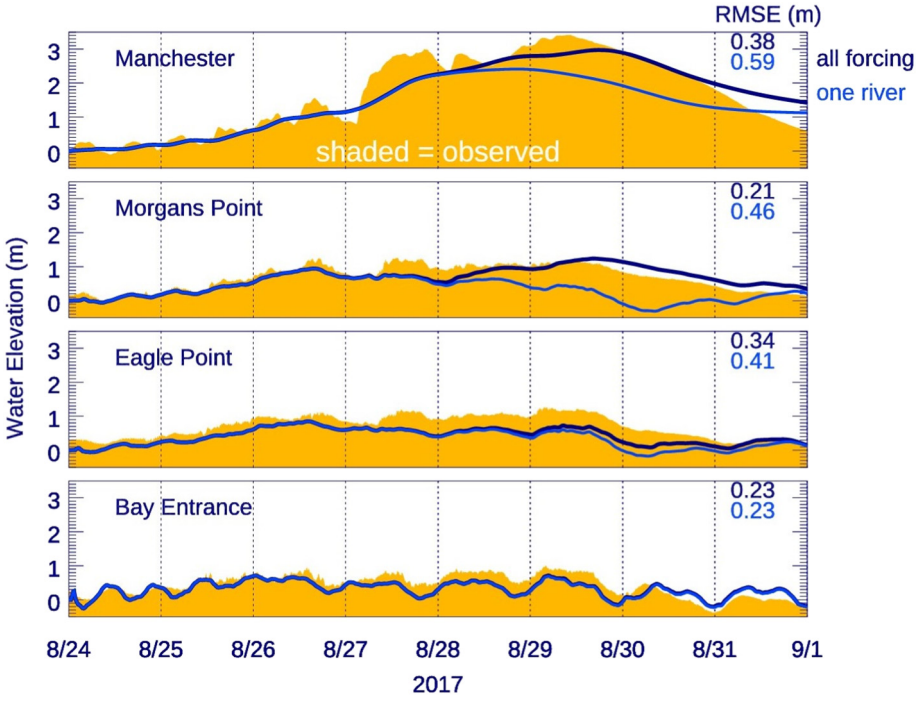

Fig. 9. Numerical results with every forcing active (darkest blue lines) and without San Jacinto River (blue lines) compared to observations at 4 NOAA sites (shaded).

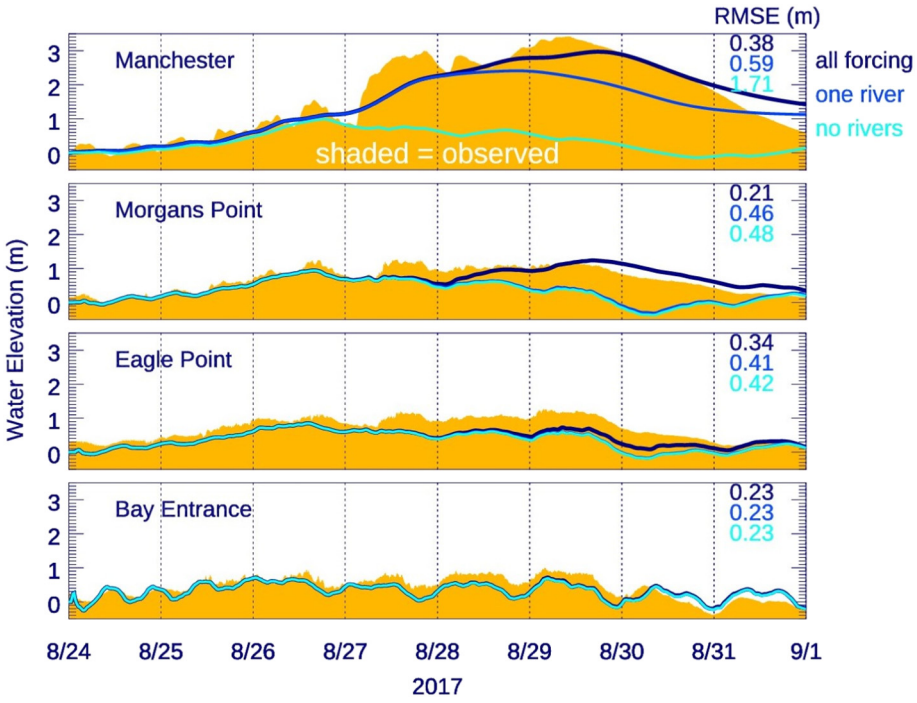

Fig. 10. Same as Figs. 8 and 9 but also with results that have no river discharge (cyan).

(Fig. 10). At Morgans Point, there was practically no difference between one river and no rivers starting on August 28th. This result indicated that the observed water level at Morgans Point, starting on August 28th, was caused mainly by flooding from the San Jacinto River. In the middle bay at Eagle Point, riverine influence was slightly noticeable beginning on August 29th as RMSE value increased by 0.01 m. In the lower bay, riverine influence was irrelevant. Overall, neglecting river input to the domain caused increased errors from the middle to the upper bay, most markedly in the Houston area.

Suppressing atmospheric forcing worsened results everywhere but the effect was secondary (Fig. 11). Around Houston, at Manchester station, atmospheric forcing was influential on August 26th and 27th only, when hurricane winds affected the estuary. This is also appreciable in the upper and middle reaches of the bay as RMSE values increased by a few cm, relative to the simulation with all forcings. Finally, eliminating forcing from ocean origin (tides and storm surge) indicated that this was most relevant in the lower and middle bay throughout the period of observations

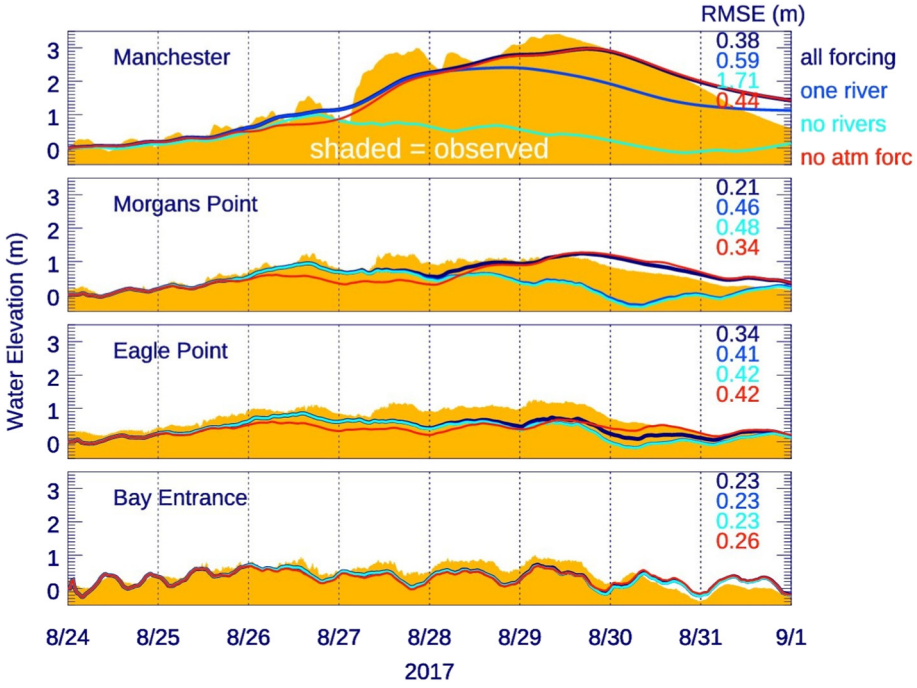

Fig. 11. Same as Figs. 8, 9 and 10 but adding a case with no atmospheric forcing (red).

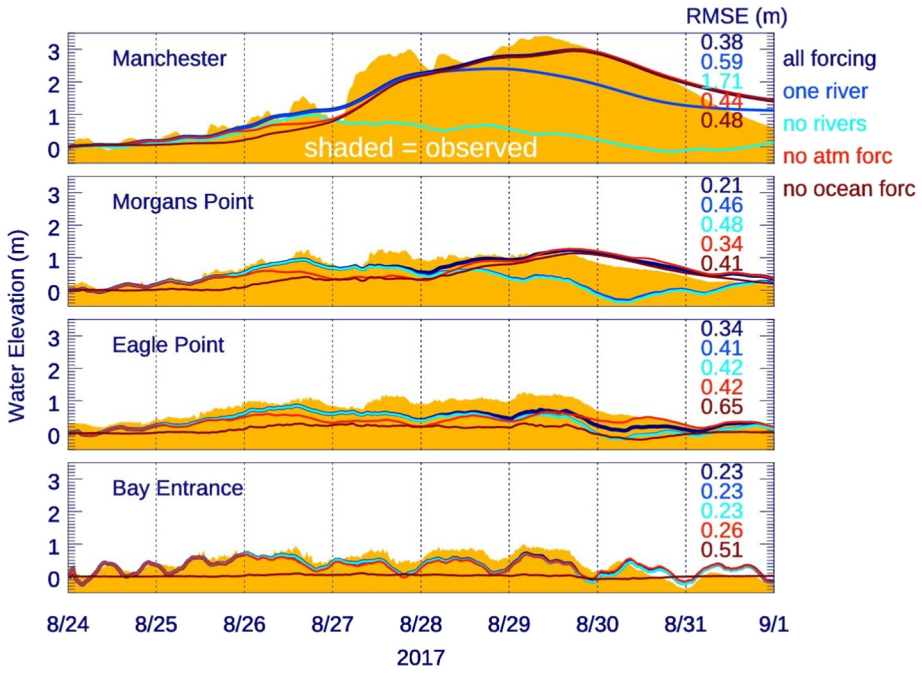

Fig. 12. Same as Figs. 8, 9, 10 and 11 but adding a case with no oceanic forcing (dark red).

(Fig. 12). Ocean forcing was also influential at the upper bay and Houston stations in the period Aug 25th–27th, when the hurricane was batting the coastal areas around Galveston Bay. Overall, the numerical results (Figs. 8–12) reinforced the hypothesis that the two rivers were critical in flooding, causing a 1–2 punch. Although the numerical simulations neglected the increased sea-level baseline in the Gulf of Mexico for 2017, it was evident that ocean forcing caused the third punch that compounded flooding.

7. Conclusion

Hurricane *Harvey* caused unprecedented flooding in and around the city of Houston in late August 2017 by dumping >1.5 m of rain in the area. Late August flooding occurred after an early-August historic storm with overnight rains of 0.15 m in the area, which made Houston's region more susceptible to flooding from *Harvey*. During the hurricane, flooding occurred from two main sources of land-derived runoff. First it was Buffalo Bayou, which runs southeastward through Houston. Then it was from San Jacinto River, which runs southward to the east of Houston. Flooding from these rivers extended for >5 days and expanded in all directions around Houston and was exacerbated mainly by 3 factors. The first factor was the phase lag between the stream cresting at Buffalo Bayou and the peak at San Jacinto River. Second, was the coastline constriction at the confluence of the two rivers, and another constriction at the expansion to the upper Galveston Bay. The first two factors were land-derived forcings. The third factor that compounded flooding was the ocean-derived forcing in the form of storm surge and an anomalously high baseline in sea level. Process-oriented numerical simulations indicated the importance of land-derived forcing in causing the flooding and the relevance of the ocean-derived forcing in determining the flooding timing. In summary, the anomalous flooding around Houston was linked to compound flooding as rivers provided a 1-2 punch and the ocean inflicted a 3rd punch.

CRediT authorship contribution statement

Arnoldo Valle-Levinson: Conceptualization, Data curation, Formal analysis, Funding acquisition, Investigation, Methodology, Software, Visualization, Writing - original draft, Writing - review & editing. **Maitane Olabarrieta:** Formal analysis, Funding acquisition, Methodology, Software, Validation, Writing - review & editing. **Lorraine Heilman:** Data curation, Methodology, Validation, Writing - review & editing.

Declaration of competing interest

The authors declare that they have no known competing financial interests or personal relationships that could have appeared to influence the work reported in this paper.

Acknowledgments

Data from USGS were obtained from their web server: *maps.waterdata.usgs.gov/mapper/index.html*. Data from NOAA were obtained from *tidesandcurrents.noaa.gov/map/index.html*. Support is acknowledged from NSF under Project OCE-1332718 to AVL and MO. MO also acknowledges support from NSF project OCE-1554892.

References

Bevacqua, E., Maraun, D., Vousdoukas, M.I., Voukouvalas, E.E., Vrac, M., Mentaschi, L., Widmann, M., 2019. Higher probability of compound flooding from precipitation and storm surge in Europe under anthropogenic climate change. Sci. Adv. 5, eaaw5531.

Chassignet, E.P., Arango, H.G., Dietrich, D., Ezer, T., Ghil, M., Haidvogel, D.B., Ma, C.-C., Mehra, A., Paiva, A.M., Sirkes, Z., 2000. DAMEE-NAB: the base experiments. Dyn. Atmos. Oceans 32, 155–183. https://doi.org/10.1016/S0377-0265(00)00046-4.

Cho, K.-H., Wang, H.V., Shen, J., Valle-Levinson, A., Teng, Y.-C., 2012. A modeling study on the response of Chesapeake Bay to hurricane events of Floyd and Isabel. Ocean Model 49–50, 22–46. https://doi.org/10.1016/j.ocemod.2012.02.005.

Cousanon, A., Sebastian, A., Morales-Napoles, O., 2018. A coupla-based Bayesian network for modeling compound flood hazardfrom riverine and coastal interactions at the catchment scale: an application to the Housto Ship Channel, Texas. Water 10, 1190.

Cousanon, A., Eilander, D., Muis, S., Veldkamp, T.I.E., Haigh, I.D., Wahl, T., Winsemius, H.C., Ward, P.J., 2020. Measuring compound flood potential from river discharge and storm surge extremes at the global scale. Nat. Hazards Earth Syst. Sci. 20, 489–504.

Du, J., Park, K., 2019. Estuarine salinity recovery from an extreme precipitation event: Hurricane Harvey in Galveston Bay. Sci. Total Environ. 670, 1049–1059.

Du, J., Park, K., Dellapenna, T.M., Clay, J.M., 2019. Dramatic hydrodynamic and sedimentary responses in Galveston Bay and adjacent inner shelf to Hurricane Harvey. Sci. Total Environ. 653, 554–564.

Emanuel, K., 2017. Assessing the present and future probability of Hurricane Harvey's rainfall. Proc. Natl. Acad. Sci. U. S. A. 114 (48), 12681–12684. https://doi.org/10.1073/pnas.1716222114.

Fritz, A., Samenow, J., 2017. Harvey unloaded 33 trillion gallons of water in the U.S. The Washington Post, September 2, 2017. https://www.washingtonpost.com/news/capital-weather-gang/wp/2017/08/30/harvey-has-unloaded-24-5-trillion-gallons-ofwater-on-texas-and-louisiana/?utm_term=.0c5e249acbb7.

Gori, A., Lin, N., Smith, J., 2020. Assessing compound flooding from landfalling tropical cyclones on the North Carolina coast. Water Resour. Res. 56, e2019WR026788. https://doi.org/10.1029/2019WR026788.

Haidvogel, D.B., Arango, H.G., Hedstrom, K., Beckmann, A., Malanotte-Rizzoli, P., Shchepetkin, A.F., 2000. Model evaluation experiments in the North Atlantic Basin: simulations in nonlinear terrain-following coordinates. Dyn. Atmos. Oceans 32, 239–281. https://doi.org/10.1016/S0377-0265(00)00049-X.

Haidvogel, D.B., Arango, H., Budgell, W.P., Cornuelle, B.D., Curchister, E., DiLorenzo, E., Fennel, K., Geyer, W.R., Hermann, A.J., Lanerolle, L., Levin, J., McWlliams, J.C., Miller, A.J., Moore, A.M., Powel, T.M., Shchepetkin, A.F., Sherwood, C.R., Signell, R.P., Warner, J.C., Wilkin, J., 2008. Regional ocean forecasting in terrain-following coordinates: model formulation and skill assessment. J. Comput. Phys. 227 (7), 3595–3624.

Horsburgh, K.J., Wilson, C., 2007. Tide-surge interaction and its role in the distribution of surge residuals in the North Sea. J. Geophys. Res. 112, C08003. https://doi.org/10.1029/2006JC004033.

Leonard, M., et al., 2014. A compound event framework for understanding extreme impacts. WIREs Clim. Change 5, 113–128.

Li, M., Zhong, L., Boicourt, W.C., Zhang, S., Zhang, D.L., 2006. Hurricane-induced storm surges, currents and destratification in a semi-enclosed bay. Geophys. Res. Lett. 33 (2), L02604. https://doi.org/10.1029/2005GL024992.

Milly, P.C.D., Wetherhald, R.T., Dunne, K.A., Delworth, T.L., 2002. Increasing risk of great floods in a changing climate. Nature 415, 514–517.

Park, K., Valentine, J.F., Sklenar, S., Weis, K.R., Dardeau, M.R., 2007. The effects of Hurricane Ivan in the inner part of Mobile Bay, Alabama. J. Coast. Res. 23 (5), 1332–1336. https://doi.org/10.2112/06-0686.1.

Proudman, J., 1957. Oscillations of tide and surge in an estuary of finite length. J. Fluid Mech. 2, 371–382.

Serafin, K.A., Ruggiero, P., Parker, K., Hill, D.F., 2019. What's streamflow got to do with it? A probabilistic simulation of the competing oceanographic and fluvial processes driving extreme along-river water levels. Nat. Hazards Earth Syst. Sci. 19, 1415–1431.

Shchepetkin, A.F., McWilliams, J.C., 2005. The regional ocean modeling system (ROMS): a split-explicit, free-surface, topography following-coordinates ocean model. Ocean Modell. 9, 347–404. https://doi.org/10.1016/j.ocemod.2004.08.002.

Valle-Levinson, A., Olabarrieta, M., Valle, A., 2013. Semidiurnal perturbations to the surge of Hurricane Sandy. Geophys. Res. Lett. 40, 1–7.

Valle-Levinson, A., Dutton, A., Martin, J.B., 2017. Spatial and temporal variability of sea level rise hot spots over the eastern United States. Geophys. Res. Lett. 44. https://doi.org/10.1002/2017GL073926.

Wahl, T., Jain, S., Bender, J., Meyers, S.D., Luther, M.E., 2015. Increasing risk of compound flooding from storm surge and rainfall for major US cities. Nat. Clim. Chang. 5, 1093–1097.

Warner, J.C., Armstrong, B., He, R., Zambon, J., 2010. Development of a Coupled Ocean-Atmosphere-Wave-Sediment Transport (COAWST) modeling system. Ocean Modell 35, 230–244. https://doi.org/10.1016/j.ocemod. 2010.07.010.

Ye, F., Zhang, Y.J., Yu, H., Sun, W., Moghimi, S., Myers, E., Nunez, K., Zhang, R., Wang, H.V., Roland, A., Martins, K., Bertin, X., Du, J., Liu, Z., 2020. Simulating storm surge and compound flooding events with a creek-to-ocean model: importance of baroclinic effects. Ocean Model. 145, 101526.

Zhang, Y.J., Ye, F., Yu, H., Sun, W., Moghimi, S., Myers, E., Nunez, K., Zhang, R., Wang, H., Roland, A., Du, J., Liu, Z., 2020. Simulating compound flooding events in a hurricane. Ocean Dyn. 70, 621–640.

Zscheischler, J., Westra, S., van den Hurk, B.J.J.M., Seneviratne, S.I., Ward, P.J., Pitman, A., et al., 2018. Future climate risk from compound events. Nat. Clim. Chang. 8, 469–477.